Systems & Control Transactions

Original Research Article
Peer Reviewed Conference Proceeding
ESCAPE 36 - European Symposium on Computer Aided Process Engineering
Sheffield, UK. 21-24 June 2026

PSE PRESS

Assessing the Impact of Solvent Recycling in Cooling Crystallization using Computer-Aided Molecular and Process Design

Gaurav Seth[a], Saman Naseri Boroujeni[a], Shubhani Paliwal[a], Amparo Galindo[a], George Jackson[a], and Claire S. Adjiman[a*]

[a] Department of Chemical Engineering, The Sargent Centre for Process Systems Engineering, Imperial College London, London SW7 2AZ, United Kingdom

* Corresponding Author: c.adjiman@imperial.ac.uk.

ABSTRACT

Although solvent-based crystallization is widely adopted for separation and purification of crystalline pharmaceutical products, solvent choice and utilisation critically influence product quality, manufacturing cost, and the environmental performance of the pharmaceutical process. Escalating demands to reduce process mass intensity (PMI), together with increasing vulnerabilities in the supply chains, necessitate the development of more efficient and resilient process designs, incorporating solvent and active pharmaceutical ingredient (API) recycling. The conceptual design of crystallization processes offers a viable route to identify flowsheets with substantially reduced solvent consumption. In this paper we present a computer-aided molecular and process design (CAMPD) formulation to explore the benefits of solvent/API recycle for two processes/APIs: (i) a continuous cooling crystallization process for mefenamic acid (MA) employing a binary solvent mixture and (ii) a batch cooling crystallization for paracetamol using a single solvent. At the conceptual design stage, the process is assumed to operate at thermodynamic equilibrium and the SAFT-γ Mie group contribution approach is used as a rigorous thermodynamic model. The optimal design for each process is determined based on the trade-off between two key performance indicators (KPIs), crystallization yield and solvent consumption. The resulting bi-objective optimization (BOO) problem is implemented in gPROMS. In addition to the solvent identities the proposed methodology also enables the simultaneous optimization of process temperatures, and the feed composition. The results demonstrate that solvents and API recycling can deliver significant benefits, leading to reduced process mass intensity (PMI) while maximizing the crystallization yield.

Keywords: Crystallization, Solvent selection, SAFT, Process design, Optimization

INTRODUCTION

Over 80% of small-molecule pharmaceuticals are delivered in crystalline form, including tablets and capsules [1]. Consequently, crystallization and purification are crucial components in pharmaceutical manufacturing. The design of isolation and purification steps impacts the physical properties of active pharmaceutical ingredients (APIs), which influence the therapeutic performance of the drug through its efficacy, absorption, and bioavailability. Additionally, crystalline form properties affect the performance of downstream operations such as filtration, drying, milling, and tableting [2].

Most industrial crystallization processes are solvent based, primarily due to the operational simplicity of such systems [3]. However, the choice of solvent(s) has a profound impact on the overall efficiency and sustainability of the crystallization process. From a thermodynamic perspective, solvent selection influences the solubility of the API, thereby affecting both the attainable crystal yield and the solvent volume required for crystallization. Moreover, solvent usage accounts for over 70% of the total energy demand and nearly 50% of the greenhouse gas emissions associated with API production [4].

Consequently, systematic approaches to solvent choice are fundamental to developing crystallization processes that are both efficient and environmentally sustainable.

Considering these challenges, increasing attention has been directed towards integration of solvent and API recycling strategies within crystallization processes [5-7]. Among these, Wong et al. [5] and Ferguson et al. [6], have carried out experimental studies on single stage, mixed-suspension, mixed-product removal (MSMPR) crystallizers with recycle and have shown that recycling mother liquor back to the crystallizer and manipulating the recycle ratio can boost the crystallization yield.

From a computer-aided design perspective, several systematic methods for integrated solvent (or solvent mixture) and process design have been reported for standalone crystallization [2, 8-11]. Various strategies have been adopted to solve such computer-aided molecular and process design (CAMPD) problems. These include generate-and-test, in which property prediction methods or databases are used to generate a list of candidate solvents to be evaluated [11], decomposition-based approach [8, 10], where optimization subproblems are used to identify molecules for which the process is further optimized; and simultaneous optimization of solvent/solvent blend and process [2, 9], where a mixed-integer nonlinear program (MINLP) is solved with respect to the process variables and the molecular structure. As expected, optimal binary solvent mixtures often results in greater solubility than pure solvents [12].

Comparatively limited attention has been given to the design of crystallization processes with solvent and API recycling. Wang and Lakerveld [7] have recently presented a continuous molecular targeting (CoMT-CAMPD) approach for solvent selection in a continuous antisolvent crystallization process. Their process configuration integrated a crystallizer with a flash drum to recycle and reuse the antisolvent. Their approach was based on the perturbed-chain statistical associating fluid theory (PC-SAFT) equation of state [13] as the underlying thermodynamic model. The resulting MINLP problem was relaxed into a sequence of nonlinear programming (NLP) problems via continuous mapping of solvent parameters.

Building on these advances, the aim of this work is to employ a simultaneous CAMPD formulation to investigate the potential benefits of solvent/API recycling for two process configurations/APIs. The first process configuration considered, Case 1, is adapted from the continuous cooling crystallization design proposed by Wang and Lakerveld [7] using a binary solvent mixture. Two solvent and API recycling strategies are examined: direct recycling of the mother liquor and recovery via a flash separation step. The performance of these recycling strategies is compared with that of standalone crystallization, with solvent identity and process operating conditions optimised in each case. The second process configuration examined, Case 2, is adapted from a laboratory-scale batch cooling crystallization setup for paracetamol using a single solvent [19]. Here pure solvent recovery is achieved via a rotary evaporator, after which the recovered solvent is reused for washing the filtered crystal cake and subsequently recycled to the crystallizer together with the fresh feed. For both case studies, the thermodynamic properties of the pure solvent and the mixtures are evaluated using SAFT-γ Mie [14].

The design approach, including the process models and design constraints for both configurations, is discussed in the next section. The results of BOO are presented in subsequently the Case studies section and the final conclusions are drawn in the last section.

DESIGN APPROACH

Problem definition

The CAMPD problem addressed in this work can be stated as: Given a crystallization process flowsheet for a pharmaceutical compound, a specified product purity, and a list of potential solvents, determine the optimal combination of solvent/solvent mixture, mixture composition and process conditions. At this stage of conceptual design, the process model is formulated based solely on thermodynamic equilibrium considerations and material balance equations.

To facilitate the formulation of the process models, a number of sets are defined as follows.

- Q denotes the set of solvents used in the process. In this work, case studies with one or two solvents are used so that $Q = \{s1, s2\}$ or $Q = \{s1\}$.
- I denotes the set of impurities present in the feed stream.
- C denotes the set of all components that may appear in any liquid stream within the process, i.e., $C = Q \cup I \cup \{API\}$, where API represents the desired product.
- $C^k \subseteq C$ represents the set of components that may appear in the solid phase.
- S represents the set of candidate solvents from which the solvents used in the process (Q) are selected.
- $\mathcal{T} = \{1, 2, \dots, N\}$ is the set of process streams, where $N = 10$ for Case 1 and $N = 22$ for Case 2.
- G is the set of functional groups used to represent the solvents in set S.

Model formulation

Continuous Cooling Crystallization – Case 1

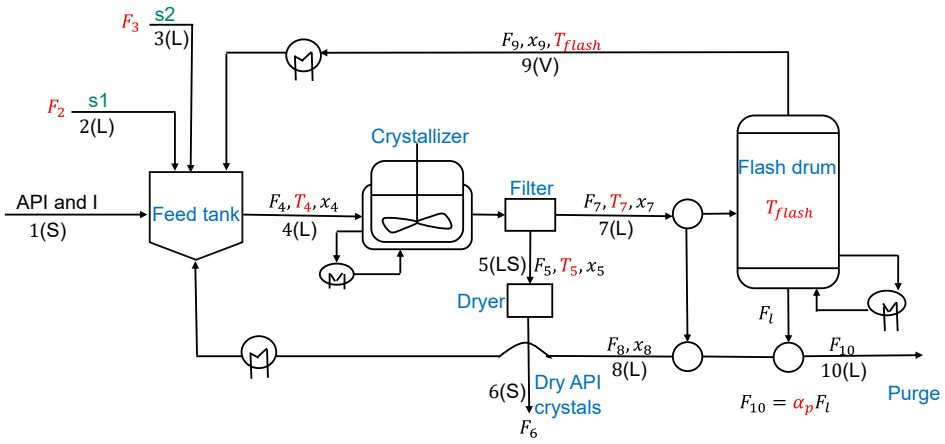

Figure 1: Flowsheet for continuous cooling crystallization of mefenamic acid. The letters L-liquid, S-solid, LS-liquid and solid, and V-vapour shown in parentheses after each stream number indicate the phases present in the corresponding process streams.

The continuous cooling crystallization flowsheet for a binary solvent mixture with solvent and API recycle via a flash drum is shown in Figure 1. The mass of component $i \in C$ in stream $t \in \mathcal{T}, M_{t,i}$, is given by

$$M_{t,i} = F_t x_{t,i} MW_i, i \in C; t \in T \tag{1}$$

where F_t is the molar flow rate of stream t, and $x_{t,i}$ represents the mole fraction of the i^{th} component in stream t, such that $\sum_{i \in C} x_{t,i} = 1, \forall t \in \mathcal{T}$.

Stream 1 is the feed entering following upstream synthesis and contains only API and impurities; hence, $x_{1,i} = 0, i \in C \backslash \{API\} \cup I$. Streams 2 and 3 correspond to pure solvent $s1$ and $s2$, respectively, $x_{2,i} = 0, i \in C \backslash \{s1\}$ and $x_{3,i} = 0, i \in C \backslash \{s2\}$. The material balance around the feed tank is given as:

$$F_1 x_{1,i} + F_2 x_{2,i} + F_3 x_{3,i} + F_8 x_{8,i} + F_9 x_{9,i} = F_4 x_{4,i}, i \in C \tag{2}$$

while that around the crystallizer and filter is given as:

$$F_4 x_{4,i} = F_5 x_{5,i} + F_7 x_{7,i}, i \in C \tag{3}$$

Stream 5 consists of the wet API cake and is modelled as a two-phase mixture of solid and liquid phases:

$$F_5 x_{5,i} = F_5^{ml} x_{5,i}^{ml} + F_5^{s} x_{5,i}^{s}, i \in C \tag{4}$$

where superscripts ml and s denote the mother liquor and solid phases, respectively. The solvent holdup in the wet cake is characterized by a mass fraction α_h:

$$\Sigma_{i \in C} M_{5,i}^{ml} = \alpha_h \left[\Sigma_{i \in C} M_{5,i}^{ml} + \Sigma_{i \in C} M_{5,i}^{s} \right] \tag{5}$$

It is further assumed that no compositional change occurs in the liquid phase during filtering; therefore, the mole fraction of mother liquor retained within the wet API cake is equal to that of the liquid stream exiting the crystallizer, stream 7, i.e., $x_{5,i}^{ml} = x_{7,i}$. Additionally, 100% impurity rejection is assumed in the crystallizer, such that only the API reaches solid–liquid equilibrium (SLE), while all impurities remain undersaturated in the mother liquor (stream 7), i.e., $x_{i,5}^{s} = 0, i \in C \backslash \{API\}$. Liquid stream 7 is at solid liquid equilibrium (SLE) with the solid APIs in stream 5, and the API solubility is calculated as:

$$\ln x_{7,API} \gamma_{7,API} = \frac{\Delta H_{API}^{m}}{R} \left(\frac{1}{T_{API}^{m}} - \frac{1}{T_7} \right) \tag{6}$$

where $\gamma_{7,API}$ denotes the activity coefficient of the API at equilibrium obtained using SAFT-γ Mie, ΔH_{API}^{m} is the molar heat of melting of the API, T_{API}^{m} is the melting temperature of the API, R is the ideal gas constant, and T_7 is the crystallizer operating temperature.

Stream 5 is sent to a dryer to produce dry API crystals (stream 6), with residual solute impurities originating from the solvent holdup within the wet cake.

Material balance around the flash drum is given as:

$$F_5 x_{5,i} = F_9 x_{9,i} + F_{10} x_{10,i} + F_8 x_{8,i}, \forall i \in C \tag{7}$$

where F_9 is vapour outlet flow rate from the flash drum. The liquid stream leaving the flash drum is split into a recycle stream (F_8) and a purge stream (F_{10}), with purge fraction defined as α_p, such that $\alpha_p = (1 - \alpha_p) F_{10} / F_8$. Phase equilibrium at the flash temperature, T_{flash} and atmospheric pressure is determined via a temperature-pressure flash (TP-flash). Furthermore, API and the impurities are assumed to be non-volatile and therefore, $x_{9,i} = 0, i \in C \backslash \{s1, s2\}$.

In some streams, at least one component in C^k should remain in the liquid phase. For a stream t, the set $\hat{C}_t^k \subseteq C^k$ of such component is defined and the solubility limit of a component $i \in \hat{C}_t^k$ is computed by assuming that only pure crystals can form (no co-crystals) [15] and by defining a hypothetical mixture with mole fraction vector $\hat{\boldsymbol{x}}_t^{(i)}$ in which the relative proportions of all components are identical to those in stream t:

$$\hat{x}_{t,i'}^{(i)}/\hat{x}_{t,s1}^{(i)} = x_{t,i'}/x_{t,s1}, i' \in C\backslash\{s1,i\};\ i \in \hat{C}_t^k;\ t \in \{4,7,8\} \quad (8)$$

with the normalization condition $\Sigma_{i' \in C} \hat{x}_{t,i'}^{(i)} = 1, i \in \hat{C}_t^k$ and component i is assumed to be at SLE:

$$\ln \hat{x}_{t,i}^{(i)} \hat{\gamma}_{t,i}^{(i)} = \frac{\Delta H_i^m}{R}\left(\frac{1}{T_i^m} - \frac{1}{T_7}\right), i \in \hat{C}_t^k; t \in \{4,7,8\} \quad (9)$$

where $\hat{\gamma}_{t,i}^{(i)}$ is the activity coefficient of component i in the hypothetical stream. The undersaturation is then imposed as:

$$x_{t,i} \leq \hat{x}_{t,i}^{(i)} - \epsilon_c, i \in \hat{C}_t^k \quad (10)$$

where ϵ_c is a small positive tolerance. These equations are applied to stream 7, where only the API crystallizes, ($\hat{C}_7^k = C^k\backslash\{API\}$), and streams 4 and 8, where no component crystallizes ($\hat{C}_4^k = \hat{C}_8^k = C^k$).

Process design constraints: Liquid range constraints are enforced so that the solvent mixture is in the liquid state in specific units:

$$T_t \leq T_{mix,t}^{bub} - T_0, \forall t \in \mathcal{T}^L \quad (11)$$

Here, T_t and $T_{mix,t}^{bub}$ are the operating temperature and the bubble-point temperature of stream t, respectively, and $\mathcal{T}^L$ is a relevant subset of $\mathcal{T}$. For continuous crystallization $\mathcal{T}^L = \{4,7\}$. Bubble-point temperatures are calculated using SAFT-γ Mie. Constraints on the melting points of the solvent(s) are not considered as the solvents have been chosen to have melting points well below the minimum process temperature. Additionally, the quaternary mixture (s1, s2, API, and l) is required to form a homogeneous liquid phase in streams $t \in \{4,7,8\}$. This is ensured by constraining a logical stability function $\phi(T_t, P_t, \boldsymbol{x}_t)$ to unity. $\phi = 1$ denotes that a TP-flash calculation at the specified conditions identifies neither a second liquid phase nor a vapour phase, while $\phi = 0$ indicates the presence of an additional fluid phase.

Switching configurations: In the equations presented so far, it is assumed that recycling using flash drum takes place. To model the direct-recycle configuration, the following constraints are introduced:

$$T_{flash} \leq Mz + T_7 + \epsilon_z \quad (12)$$

$$T_{flash} \geq T_7 + \epsilon_z(1-z) \quad (13)$$

$$T_{flash} \geq zT_{mix,7}^{bub} + \epsilon_z \quad (14)$$

ϵ_z is a small positive constant, M is a large positive constant, z parameter indicating the status of the flash drum: (active for $z = 1$, in-active for $z = 0$). denotes a binary parameter indicating the operating status of the flash drum.

Batch Cooling Crystallization – Case 2

Figure 2 depicts the batch cooling crystallization process. The crystallization is performed in a pure solvent and is followed by filtration, washing and drying. Due its batch nature, the process requires a few iterations to reach a steady state. While this is considered via a batch index b and a total number of batches N_b, the detailed dynamics of the process units are neglected at the conceptual design stage. Each unit is modelled by considering the initial time (inlet) and final time (outlet). As a result, the mass balances and phase-equilibrium formulations for the crystallizer, filter, and dryer are analogous to those described previously (with the addition of the batch index b) and are not repeated here.

As in the continuous crystallization model, 100% impurity rejection is assumed during batch crystallization. Specifically, only the API is allowed to reach SLE, while impurities are constrained to remain undersaturated in the relevant mother liquor streams (Streams 1, 2, 5, 17, 18, and 22). Furthermore, temperature constraints are also imposed for streams $t \in \mathcal{T}^L = \{1,2\}$ (cf. Eq. (11)). After filter 1, the cake is washed using a fraction of pure solvent from the solvent recovery tank. The mass of wash solvent in batch b, M_{14}^b is modelled using wash mass fraction, α_w:

$$M_{14}^b = \alpha_w M_{3,API}^{s,b} \quad (15)$$

where $M_{3,API}^{s,b}$ denotes the mass of solid API in stream 3.

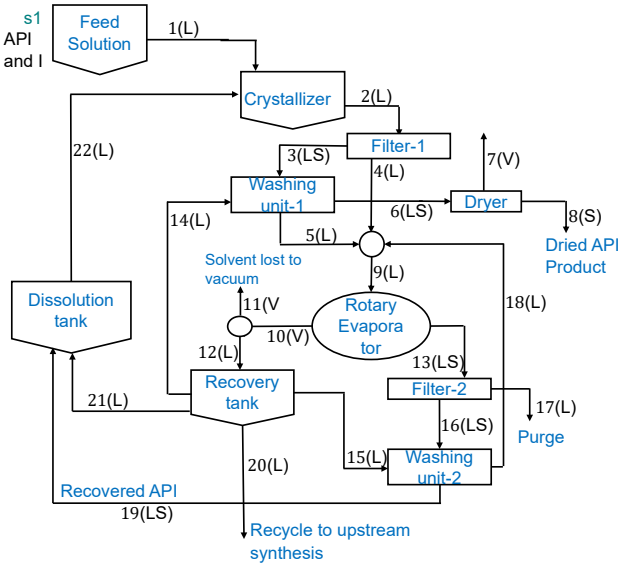

Figure 2: Flowsheet for Batch cooling crystallization

The washing operation is assumed to occur at room temperature (i.e., $T_5^b = T_5 = 293$ K) with the resulting mother liquor is at solid-liquid equilibrium (SLE) with respect to the API. Accordingly, API solubility in stream 5 is given by:

$$\ln x_{5,API}^b \gamma_{5,API}^b = \frac{\Delta H_{API}^m}{R}\left(\frac{1}{T_{API}^m} - \frac{1}{T_5}\right) \quad (16)$$

The resulting liquid streams from filter 1 (stream 4) and washing units 1 and 2 are combined and fed to a

rotary evaporator, where a mass fraction, α_{evap}, of the total solvent amount in the combined stream (stream 9) is evaporated and collected in the solvent recovery tank. The corresponding mass balances are given by

$$M^b_{9,i} = M^b_{5,i} + M^b_{4,i} + M^b_{18,i}, i \in C \quad (17)$$

$$M^b_{10} = \alpha_{evap} M^b_{9,s1} = M^b_{11} + M^b_{12} \quad (18)$$

$$M^b_{11} = \alpha_c M^b_{10} \quad (19)$$

where α_c represents the fraction of evaporated solvent lost in the vacuum system. For clarity, the component index i is omitted for the streams containing pure solvent. The concentrated mother liquor leaving the rotary evaporator is cooled to room temperature ($T^b_{13} = T_{13} = 293$ K) and sent to filter unit 2 to recover additional API. The filter cake is washed using solvent from the solvent recovery tank at room temperature. Next, the washed cake is redissolved and recycled to the crystallizer. The filtrate is discarded (stream 17) whereas the wash liquor (stream 18) is recycled back to the evaporator.

The composition of the recycle stream (stream 22) is constrained such that the mass ratio of API to the solvent is identical to that of the fresh feed stream. i.e.,

$$M^b_{API,22}/M^b_{s1,22} = M^b_{API,1}/M^b_{s1,1} \quad (20)$$

This ensures consistent feed composition upon recycle.

Design Constraints and MINLP formulation

Additional constraints and model equations are required to describe the selection of a solvent from the set of candidates S and to quantify process performance.

Solvent assignment constraints: Logical constraints are imposed on the binary variables representing the choice of solvent. Exactly one solvent from set candidate S is assigned to the solvent component(s).

$$\Sigma_{s \in S} y_{q,s} = 1, \forall q \in Q \quad (21)$$

For continuous cooling crystallization configuration, $Q = \{s1, s2\}$, whereas for batch cooling crystallization, $Q = \{s1\}$. To prevent the same candidate solvent from being assigned to both solvent components in a binary solvent mixture, the following constraint is imposed:

$$\Sigma_{q \in Q} y_{q,s} \leq 1, \forall s \in S \quad (22)$$

Since thermodynamic properties are computed using a group contribution approach, each solvent candidate s is represented by a set of functional groups $n_{s,k}$, where k is a functional group in set G. The solvents $q \in Q$ are then defined as:

$$\tilde{n}_{q,k} = \Sigma_{s \in S} y_{q,s} n_{s,k}, \forall q \in Q, \forall k \in G \quad (23)$$

where $\tilde{n}_{q,k}$ denotes the number of functional group of type k present in solvent q.

KPIs: The KPIs considered in this work are process mass intensity (PMI), product purity, and crystal yield.

- PMI is sustainability metric that quantifies material efficiency. For continuous crystallization process, it is calculated as:

$$PMI = \Sigma_{t \in \{1,2,3\}} \Sigma_{i \in C} M_{i,t} / M_{API,6}\,, \quad (24)$$

For batch crystallization, the overall PMI is evaluated over N_b batches by accounting explicitly for the solvent recovered and recycled to upstream synthesis:

$$PMI = \left(\Sigma^{N_b}_{b=1}\left(\Sigma_{i \in C} M^b_{i,1} - M^b_{s1,20}\right)\right) / \Sigma^{N_b}_{b=1} M^b_{API,8} \quad (25)$$

- Product purity (PP) is defined as the fraction of desired product in the dry API stream. For continuous crystallization process this is defined as

$$PP = M_{API,6} / (M_{API,6} + M_{I,6}) \times 100 \quad (26)$$

An analogous expression is used for batch crystallization process. In this work, product purity is imposed as a constraint, with minimum target value set to 99.5%.

- Crystal yield ($Y_c, \%$) is the mass fraction of API recovered in the product stream relative to that in the feed. For the continuous crystallization process, the yield:

$$Y_c = (M_{API,6} / M_{API,1}) \times 100 \quad (27)$$

For batch crystallization, the yield is defined over N_b batches and calculated as:

$$Y_c = \Sigma^{N_b}_{b=1} M^b_{API,8} / (N_b M^b_{API,1}) \quad (28)$$

Crystal yield is also constrained, with a minimum value of 90% imposed for both the systems.

CASE STUDIES

To understand the trade-offs between crystal yield and material consumption, a BOO-CAMPD formulation is constructed to simultaneously minimize the PMI and maximize the yield. It is solved using the ϵ-constraint method [16], reformulating a series of single level optimization problems, each maximizing crystal yield subject to a specified upper bound (ϵ_{PMI}) on PMI. The formulation is implemented in gPROMS Process, version 2023.1.0.

The optimization problem is solved using OAREAP, the implementation of the outer approximation algorithm [17] in gPROMS. To increase the likelihood of finding the global solution, the NLP primal subproblems are solved using a multi-start strategy, with 16 initial guesses, and the NLPMSO local solver.

Continuous Cooling Crystallization – Case 1

The continuous cooling crystallization of mefenamic acid (MA), with toluic acid (TA) as an impurity is

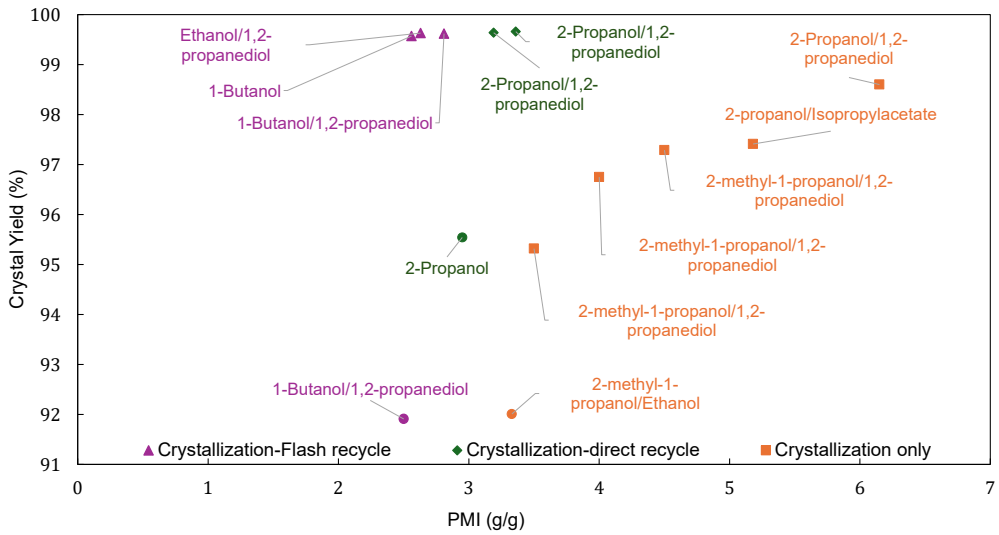

Figure 3: Pareto-optimal solutions for continuous crystallization of mefenamic acid, showing the optimal solvent/solvent pairs obtained for different cases.

investigated. Since all analyses are performed on relative basis, stream 1 is assigned a total molar flow of 1 mol/s, with an impurity to API weight ratio of $1:30$. The identity and composition of the binary solvent mixture, and the process operating conditions, are optimized in an integrated manner. The decision variables, their bounds, and the set of 15 candidate solvents are shown in Table 1. The candidates are selected based on the availability of the required SAFT-γ Mie interaction parameters [18]. The optimization problem is solved for three configurations: crystallization with direct recycle, crystallization with flash recycle, and stand-alone crystallization. For all cases, the minimum allowable PMI is fixed at 2.5 g/g, to avoid the formation of highly viscous slurries. Upper bound on PMI is varied to generate multiple instances of the ϵ-constraint formulation for maximizing crystal yield.

Table 1: Case 1: decision variables and bounds

Variables	Range
$y_{q,s}$	{0, 1}
F_2, F_3(moles/s)	[0, 1000]
T_4, T_7(K)	[290, 360]
T_{flash}	[290, 420]
α_p	[0.2, 0.9]
S	{water, acetic acid, cyclohexanone, acetone, ethanol, methanol, butanol, pentanol, 2-propanol, 1, 2-propanediol, 2-methyl-1-propanol, ethyl acetate, butyl acetate, isobutyl acetate, isopropyl acetate}

The ϵ_{PMI} values are varied between the PMI at the solution of the minimization of PMI solution and the PMI at maximum yield. For stand-alone crystallization (crystallization only in Figure 3) case, ϵ_{PMI} values are set at intervals of 0.5 between these bounds. For both recycling cases, ϵ_{PMI} values are set with an increment of 0.2. The Pareto-optimal solutions for the three configurations are compared in Figure 3, where the optimal solvent(s) corresponding to each solution are also reported along with the associated PMI and yield values. For certain solutions, only one solvent is reported as the optimal flow rate of the second solvent is zero, implying that a pure-solvent is optimal at those conditions. The circled points denote the solutions corresponding to the minimum PMI.

For most solutions, the temperature range attains its maximum value ($T_4 = 360$ K, $T_7 = 290$ K), reflecting the increased solubility range needed to enhance API recovery. Further, the purge ratio (α_p) is driven to lower bound of 0.2 corresponding to the maximum allowable recycle to the crystallizer.

As expected, increasing the PMI results in higher solvent usage and process yield. Incorporating a recycle stream retains API within the process and reduces the fresh solvent demand, thereby enhancing crystal yield without proportionately increasing PMI. This is seen as a narrower range of PMI values on the Pareto front and a decrease in the number of Pareto-optimal solutions. The range of PMI values is narrowest with the use of flash drum as this reduces the fresh solvent requirement.

Batch Cooling Crystallization – Case 2

Batch cooling crystallization of paracetamol with metacetamol and acetanilide as impurities is studied. The feed contains 16.5 g of paracetamol, corresponding to the laboratory scale to which this process is based, with an impurity to API weight ratio of $1:30$ for both impurities. The design objective is to determine the optimal solvent,

solvent mass, and process conditions that maximize the crystal yield while minimizing PMI. The decision variables and the variable bounds are detailed in Table 2. The details of the SAFT-γ Mie model used for paracetamol is given in the supplementary material.

The crystallization process is examined over $N_b = 20$ batches, with overall PMI constrained to a lower bound of 2.2 g/g. Multiple ϵ-constraint optimization instances are generated by varying the upper bound on PMI to maximize crystal yield. The resulting BOO-CAMPD optimal solutions are presented in Figure 4. Three Pareto-optimal solutions are shown as points with $b = 1, \ldots, 20$. Ethanol yields the minimum overall PMI, while isopropyl acetate yields the maximum crystal yield. The range of operating temperatures is maximized in all cases ($T_1 = 343$ K, $T_2 = 263$ K). Similar to the continuous crystallization case, a narrow Pareto front is observed for the batch crystallization process.

Table 2: Case 2: decision variables and bounds

Variables	Range
$y_{q,s}$	{0, 1}
$M_{s1,1}$ (g)	[0, 1000]
T_1, T_2(K)	[263, 343]
α_{evap}	[0, 0.8]
$\alpha_h, \alpha_w, \alpha_c$	0.25, 0.5, 0.1
S	{water, acetic acid, acetone, ethanol, methanol, butanol, pentanol, 2-propanol, 1, 2-propanediol, 2-methyl-1-propanol, ethyl acetate, butyl acetate, isobutyl acetate, isopropyl acetate}

The variation of PMI and crystal yield with the number of batches is also examined in Figure 4. As the Pareto-optimal solutions transition from minimum PMI (ethanol) to maximum yield (isopropyl acetate), the number of batches required to reach steady state decreases. In the case of isopropyl acetate, the changes in both PMI and yield with batch number are negligible. This behaviour arises because a large amount of solvent is used in the first batch, leading to maximum product recovery during crystallization. Consequently, very little material is available for recycle, thereby leading to minimal variation across batches. In other cases, the introduction of recycling leads to simultaneous improvement in crystal yield and PMI. Overall, the Pareto front moves closer to the utopia point as b increases.

CONCLUSIONS

We have presented a systematic methodology for the identification of optimal solvent/solvent mixtures, and process conditions for integrated crystallization and solvent/API recovery processes. A general CAMPD framework was formulated to design the crystallization processes and was applied to a continuous crystallization process for mefenamic acid and a batch crystallization process for paracetamol. Both processes incorporate solvent and API recovery and recycle. The process models were based on rigorous thermodynamics and the imposition of a number of thermodynamic constraints. The results have demonstrated the potential benefits of solvent recycling. This is reflected by a narrowing of the Pareto front upon the introduction of a recycle stream in the continuous case, indicating that improvements in crystal yield can be achieved with only marginal increases in PMI. In the batch case, this is seen as the Pareto front moves closer to the utopia after a small number of batches.

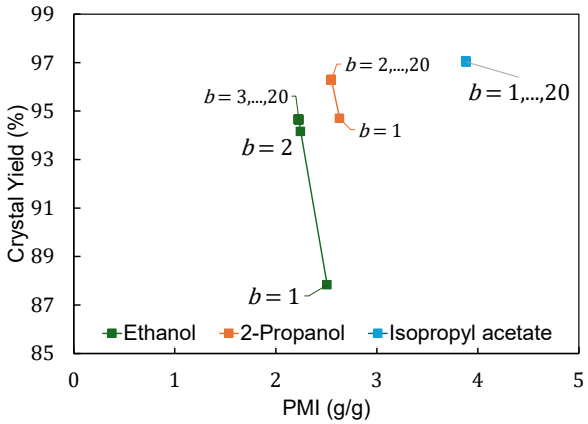

Figure 4: Pareto-optimal solutions obtained for paracetamol batch crystallization, showing the variation in PMI and crystal yield as a function of batch cycle b.

These results confirm that low-PMI operation can be realized while maintaining high levels of product recovery. Despite the sustainability advantages of recycling, the case studies also indicate that solvent selection plays a critical role and recycle may offer limited benefits for certain solvents. Integrating energy consumption into the multi-objective optimization framework will enable a more comprehensive sustainability assessment and facilitate the identification of solvent–process combinations that balance material efficiency with energy efficiency.

DIGITAL SUPPLEMENTARY MATERIAL

The supplementary material is available at LAPSE Id: **LAPSE:2026.0014**.

ACKNOWLEDGEMENTS

The authors gratefully acknowledge funding from the UK Engineering and Physical Sciences Research Council (EPSRC) research grant (EP/W01923X/1 and EP/Z532964/1).

AUTHOR IDENTIFIERS

Author ORCIDs:
Seth G: 0009-0006-3466-9345
Naseri S: 0000-0003-2830-8624
Paliwal S: 0000-0002-1993-591X
Jackson G: 0000-0002-8029-8868
Galindo A: 0000-0002-4902-4156
Adjiman CS: 0000-0002-4573-7722

REFERENCES

1. Variankaval N, Cote AS, Doherty MF. From form to function: crystallization of active pharmaceutical ingredients. AIChE Journal 54:1682-1688 (2008). https://doi.org/10.1002/aic.11555
2. Watson OL, Jonuzaj S, McGinty J, Sefcik J, Galindo A, Jackson G, Adjiman CS. Computer aided design of solvent blends for hybrid cooling and antisolvent crystallization of active pharmaceutical ingredients. Org. Process Res. Dev. 25:1123-1142 (2021). https://doi.org/10.1021/acs.oprd.0c00516
3. Tung H, Paul EL, Midler M, McCauley JA. Crystallization of organic compounds. Wiley (2023). https://doi.org/10.1002/9781119879497
4. Gani, R., Jimenez-Gonzalez, C., ten Kate, A., Crafts, P.A., Jones, M., Powell, L., Atherton, J.H. and Cordiner, J.L., 2006. A modern approach to solvent selection: although chemists' and engineers' intuition is still important, powerful tools are becoming available to reduce the effort needed to select the right solvent. Chemical Engineering, 113(3), pp.30-44.
5. Wong SY, Tatusko AP, Trout BL, Myerson AS. Development of continuous crystallization processes using a single-stage mixed-suspension, mixed-product removal crystallizer with recycle. Crystal Growth & Design 12:5701-5707 (2012). https://doi.org/10.1021/cg301221q
6. Ferguson S, Ortner F, Quon J, Peeva L, Livingston A, Trout BL, Myerson AS. Use of continuous MSMPR crystallization with integrated nanofiltration membrane recycle for enhanced yield and purity in API crystallization. Crystal Growth & Design 14:617-627 (2013). https://doi.org/10.1021/cg401491y
7. Wang J, Lakerveld R. Integrated solvent and process design for continuous crystallization and solvent recycling using PC?SAFT. AIChE Journal 64:1205-1216 (2017). https://doi.org/10.1002/aic.15998
8. Karunanithi AT, Achenie LEK, Gani R. A computer-aided molecular design framework for crystallization solvent design. Chemical Engineering Science 61:1247-1260 (2006). https://doi.org/10.1016/j.ces.2005.08.031
9. Watson, O.L., Galindo, A., Jackson, G. and Adjiman, C.S., 2019, November. Computer-Aided Design of Solvent Blends for the Cooling and Anti-Solvent Crystallization of Active Pharmaceutical Ingredients. In 2019 AIChE Annual Meeting. AIChE.
10. Karunanithi AT, Acquah C, Achenie LEK, Sithambaram S, Suib SL. Solvent design for crystallization of carboxylic acids. Computers & Chemical Engineering 33:1014-1021 (2009). https://doi.org/10.1016/j.compchemeng.2008.11.003
11. Foli? M, Gani R, Jiménez-González C, Constable DJC. Systematic selection of green solvents for organic reacting systems. Chinese Journal of Chemical Engineering 16:376-383 (2008). https://doi.org/10.1016/s1004-9541(08)60092-0
12. Jonuzaj S, Akula PT, Kleniati P, Adjiman CS. The formulation of optimal mixtures with generalized disjunctive programming: a solvent design case study. AIChE Journal 62:1616-1633 (2016). https://doi.org/10.1002/aic.15122
13. Gross J, Sadowski G. Application of perturbation theory to a hard-chain reference fluid: an equation of state for square-well chains. Fluid Phase Equilibria 168:183-199 (2000). https://doi.org/10.1016/s0378-3812(00)00302-2
14. Haslam AJ, González-Pérez A, Di Lecce S, Khalit SH, Perdomo FA, Kournopoulos S, Kohns M, Lindeboom T, Wehbe M, Febra S, Jackson G, Adjiman CS, Galindo A. Expanding the applications of the saft-? mie group-contribution equation of state: prediction of thermodynamic properties and phase behavior of mixtures. J. Chem. Eng. Data 65:5862-5890 (2020). https://doi.org/10.1021/acs.jced.0c00746
15. Muhieddine MH, Viswanath SK, Armstrong A, Galindo A, Adjiman CS. Model-based solvent selection for the synthesis and crystallisation of pharmaceutical compounds. Chemical Engineering Science 264:118125 (2022). https://doi.org/10.1016/j.ces.2022.118125
16. Laumanns M, Thiele L, Zitzler E. An efficient, adaptive parameter variation scheme for metaheuristics based on the epsilon-constraint method. European Journal of Operational Research 169:932-942 (2006). https://doi.org/10.1016/j.ejor.2004.08.029
17. Viswanathan J, Grossmann IE. A combined penalty function and outer-approximation method for MINLP optimization. Computers & Chemical Engineering 14:769-782 (1990). https://doi.org/10.1016/0098-1354(90)87085-4
18. Febra SA, Bernet T, Mack C, McGinty J, Onyemelukwe II, Urwin SJ, Sefcik J, ter Horst JH,

Adjiman CS, Jackson G, Galindo A. Extending the saft-? mie approach to model benzoic acid, diphenylamine, and mefenamic acid: solubility prediction and experimental measurement. Fluid Phase Equilibria 540:113002 (2021). https://doi.org/10.1016/j.fluid.2021.113002

19. Scott A. Brown, Yusuf Khan, Nicola Voiculescu, Anna Jawor-Baczynska, Kirstie Milne, Jorge Calderon De Anda, Helen P. Wheatcroft, Christopher Burcham, Stanley Kolis, Jun Li, Jan Sefcik and Chris J. Price. Enhancing Product Yield, Purity & Sustainability by API & Solvent Recycling in Cooling Crystallisation. Under review.